Published in final edited form as:
*NMR Biomed*. 2011 July ; 24(6): 582–591. doi:10.1002/nbm.1644.

# Imaging pH and Metastasis

**Arig Ibrahim Hashim**[*], **Xiaomeng Zhang**[*], **Jonathan W. Wojtkowiakk**, and **Robert J. Gillies**
Department of Imaging research H. Lee Moffitt Cancer Center and Research Institute 12902 Magnolia Dr. Tampa, FL 33612

## Abstract

Metastasis is a multistep process that culminates in the spread of cells from a primary tumor to a distant site or organs. For tumor cells to be able to metastasize, they have to locally invade through basement membrane into the lymphatic and the blood vasculatures. Eventually they extravasate from the blood and colonize in the secondary organ. This process involves multiple interactions between the tumor cells and their microenvironments. The microenvironment surrounding tumors has a significant impact on tumor development and progression. A key factor in the microenvironment is an acidic pH. The extracellular pH of solid tumors is more acidic in comparison to normal tissue as a consequence of high glycolysis and poor perfusion. It plays an important role in almost all steps of metastasis. The past decades have seen development of technologies to non-invasively measure intra- and/or extracellular pH. Most successful measurements are MR-based, and sensitivity and accuracy have dramatically improved. Quantitatively imaging the distribution of acidity helps us understand the role of the tumor microenvironment in cancer progression. This review discusses different MR methods in measuring tumor pH along with emphasizing the importance of extracelluar tumor low pH on different steps of metastasis; more specifically focusing on Epithelial to Mesenchymal transition (EMT), and anti cancer immunity.

### Keywords

Tumor pH; Metastasis; Tumor microenvironment

Metastasis and its sequelae are the leading causes of cancer morbidity and mortality. As shown in FIGURE 1, metastasis involves a series of discrete steps from local invasion and intravasation through to extravasation and colonization (1). Despite intense research over the past few decades, defining the exact molecular mechanisms involved in these steps has remained elusive. Defining metastasis is made more difficult by the large molecular heterogeneity and redundancy in these pathways, combined with the low probability of forming successful metastatic lesions. In typical experimental settings, up to 500,000 cancer cells are injected intraveneously, which leads to the formation of only 50 or 100 metastatic lesions. In aggressive metastatic human cancers, there can be up to 23 million circulating tumor cells at any one time (2).

The physical microenvironment of tumors (pH, $pO_2$) can have a great impact on the successful formation of metastasis. Solid tumors are believed to contain volumes that are highly acidic (3). This low extracellular pH (pHe) has been associated with tumorigenic

Corresponding author: Robert J. Gillies, PhD Vice-chair Radiology and Director, Experimental Imaging Program, H. Lee Moffitt Cancer Center and Research Institute. 12902 Magnolia Dr. SRB-2 Tampa, FL 33612 (813) 745-8355 robert.gillies@moffitt.org.
[*]these authors contributed equally to this work

transformation, chromosomal rearrangements, extracellular matrix breakdown, increased migration and invasion, and induction of growth factors and proteases (4,5).

Tumor acidity is a consequence of high rates of glucose metabolism, combined with poor perfusion. Experimentally induced hyperglycemia acidifies the tumor microenvironment (6-8) coincident with an increase in the glycolytic rate (9) which can lead to a reduction in extracellular pH, pHe, from 7.4 to 6.7 (10). The end product of fermentative glucose metabolism is lactate, and tumor lactate levels are independently correlated with metastasis, low pH and reduced survival (11,12). However, low pH is not equivalent to lactate, as the hydrogen ion in glycolysis is released at an earlier enzymatic step, namely glyceraldehyde phosphate dehydrogenase, GAPdH. Additionally, movement of carbons through the pentose phosphate pathway can also produce acids. Studies with glycolysis-deficient cells indicate that Embden-Meyerhoff glycolysis is not the only source of extracellular acid in solid tumors. $CO_2$ may be a significant source of acid, as oxidative energy metabolism results in the production of the volatile acid $H_2CO_3$ from $CO_2$ might lead to a net $H^+$ production within a solid tumors (13). Furthermore $CO_2$ , may be derived from elevated glutaminolysis (14). A wealth of research evidence showed that acidosis is caused by reactions other than lactate production. In muscles the increased lactate production is coincides with cellular acidosis and remain a good indirect marker for cell metabolic conditions that include metabolic acidosis (15).

Poor perfusion in tumors no only reduces the ability to remove tumor-derived acid; it also leads to regional hypoxia, which can exacerbate fermentative metabolism. It has been proposed that this leads to selection for cells that are resistant to acid and hypoxia-mediated toxicities (16). Notably, hypoxia leads to expression of carbonic anhydrase IX and the sodium-hydrogen exchanger, which can promote the movement of intracellularly produced $H^+$ to the extracellular space (17).

Finally, it must be appreciated that lactate and acidity may be uncoupled also in their effects on cancer cells. As described above, acidosis can occur with or without high lactic acid. Lactate dehydrogenase, LDH-A, and the glucose transporter, GLUT-1, are both regulated by hypoxia via the transcription factor, HIF-1α. As a consequence, tumor cells can produce lactate and co-transport it along with $H^+$, leading to maintenance of $pH_i$ and a lowering of the tumor $pH_e$, yet these products can also be transported independently. Gene expression studies using primary human mammary epithelial cells suggest that lactic acidosis and general (HCl) acidosis trigger similar genetic responses, which are distinct from genetic responses to lactate and hypoxia (18). Furthermore, lactate can be a potent transcriptional regulator, even in the absence of acidosis. For example, it has been shown to stabilize and lead to elevated HIF-1α levels (19).

In this review, we will briefly discuss MR-based methods for measuring tumor pH, which was recently reviewed (20,21), and then discuss evidence relating tumor acidity to promotion of metastasis.

## Imaging pH with MR

### Magnetic resonance spectroscopy (MRS)

MRS and magnetic resonance spectroscopy imaging (MRSI) can provide accurate and precise noninvasive measures of pH *in vivo* with reasonable spatial resolution. An ideal MR pH indicator should have the following criteria: large pH sensitivity, a pKa in the physiological range, non-toxic at useful concentrations, metabolically stable and provide a high SNR within a short time period. Both endogenous and exogenous NMR-active compounds have been used to measure pH in vivo (TABLE 1). Measuring pH with MRS/

MRSI is generally based on a difference in chemical shifts between pH-dependent and independent resonances. If they are in the same compartment, protonation reactions are in fast exchange, and thus the chemical shift can be use to predict the pH. If there are intervening membranes, exchange is slow and compounds at different pHs will resonate at distinct frequencies, giving rise to multiple peaks.

**$^{31}$P—**Phosphorous is an abundant and sensitive MR active nucleus. The $^{31}$P isotope is 100% natural abundance, and $^{31}$P spectra exhibit a wide variety of compounds. Many small phosphorylated metabolites exist within cells have concentrations in the range of 0.1-10 mM. The most significant NMR-visible endogenous phosphorous signals from mammalian tissues come from NTPs, inorganic phosphate (Pi), and phosphocreatine (PCr). $^{31}$P MRS provides a noninvasive technique for simultaneously measuring intracellular pH, pHi, from the chemical shift of endogenous Pi and $pH_e$ from the chemical shift of exogenous indicators, such as 3-aminopropyl phosphonate (3-APP) (22). In tumors, the chemical shift of Pi, with a pKa ≈ 6.8, is usually referenced to that of glycerophosphoryl choline (at 0.49 ppm); or α peak from NTP (at −10.05 ppm), and the resulting frequency can be used to estimate pH within 0.05 pH unit after correction. Numerous studies have shown that the Pi measured by in vivo MRS is primarily intracellular and thus, the resonance frequency of this nucleus provides a measure of the intracellular pH (pHi). This has been confirmed by comparing the pH measured by Pi to that measured by intracellulary trapped 2-deoxy glucose 6-phosphate (23,24). These and subsequent studies have shown that pHi of tumors remains neutral to alkaline, even when the extracellular tumor pH is acidic (20). In order to measure pHe by MRS, it is necessary to introduce an exogenous reagent. Although a number of phosphonate-based probes have been developed for measurement of pH, only a few have demonstrated their qualities. Phenylposphonic acid has been used as a $^{31}$P-MRS indicator of extracellular pH in perfused tissues (25). Szwergold has also developed a number of phosphonate-based probes, some of which were reported to be extracellular (26). 3-APP is an exogenous indicator widely used to measure the pHe of tumors in animal models. It was developed in 1994 and shown to be nontoxic and membrane impermeant. These studies and others simultaneously measure the pHe and pHi in bioreactors and *in vivo* using the frequencies of 3-APP and Pi, respectively (27) (FIGURE 2). This approach has been used by numerous groups to measure the pHi and pHe in a variety of tumor xenograft models (28). These studies have demonstrated unequivocally that the pHe of tumors is significantly more acidic than that of normal tissues.

**$^{19}$F MRS—**Similar to $^{31}$P, $^{19}$F can also measure a pH-induced chemical shift, but with higher sensitivity and less compartment artifacts. Hunjan and Mason developed fluorinated vitamin B6 derivatives as $^{19}$F NMR pH indicators that readily across cell membrane providing the measurement of pHi and pHe gradient in vivo (29). Griffiths et al compared 19F probe, 3-[N-(4-fluor-2-trifluoromethylphenyl)-sulphamoyl]-propionic acid (ZK-150471) with 3-APP in three solid tumor type and yields consistent pHe values (30). A drawback common to both $^{19}$F and $^{31}$P, however, is that MRS is limited in spatial resolution, even at high field.

**$^{1}$H MRSI—**Protons are the most abundant and sensitive NMR-active isotope in biological systems. Their sensitivity derives from their high gyromagnetic ratio and isotopic abundance. The most predominant peak in the NMR spectrum comes from the 110 molar protons found in water. However, with solvent suppression techniques, the water resonance can be reduced and $^{1}$H resonances from metabolites and indicators can be measured. Thus, compared to $^{31}$P, $^{1}$H MRS allows for data to be collected in smaller voxels in less time. In general, $^{1}$H MRS approaches to measure tumor $pH_e$ have relied on compounds, such as imidazoles and aromatics, which resonate at higher frequencies (downfield) compared to

endogenous metabolites. Rabenstein and Isab first proposed using imidazoles as extrinsic $pH_e$ indicators in 1982 (31). Ballesteros and colleagues have suggested several modifications of the basic structure of the imidazole molecule to improve its performance as an extrinsic pH probe (32). The most popular exogenous imidazole for 1H NMR-sensitive pHe indicator is the pH-sensitive H2 resonance of 2-imidazole-1-yl-3-ethoxycarbonyl propionic acid (IEPA), which has been shown to be non-toxic and to remain extracellular (33). Using magnetic resonance spectroscopic imaging, IEPA has been used to measure pHe in breast cancer tumors and gliomas with spatial resolution up to $1 \times 1 \times 1$ $mm^3$ (FIGURE 3). García-Martín *et al.* compared the pHe map generated from IEPA MRSI and distribution of metabolites in C6 gliomas to investigate the correlations of pHe and lactate (34). This strategy has been improved by introducing new imidazol probe ISUCA [(±)2-(imidazol-1-yl)succinic acid] which had less effects on tumor metabolism (35). These studies showed that the tumor pHe was heterogeneous, with differences of as much as 0.5 pH units across 8 mm in distance. The relationship between the low $pH_e$ and perfusion has been inferred through co-registration with contrast-enhanced images, yet cannot be directly tested by this method.

**Hyperpolarized $^{13}C$ bicarbonate—**Although previous isotopes have good pH-sensitive chemical shift dispersion, many others are limited by low sensitivities due to low magnetic energy of nuclear spins at room temperature, even at the high magnetic field. For example, carbon-13 is intrinsically low sensitivity as it has only 1.1% naturally abundant. Hoffman and Henkens have shown that $^{13}C$ had potential to estimate intracellular $CO_2$ hydration and $HCO_3^-$ dehydration (36). Arus et al. have investigated pH of superfused frog muscle with natural abundance $^{13}C$ MRS with a high concentrations of labeled bicarbonate (37). The sensitivity of these applications can be dramatically improved by dynamic nuclear hyperpolarization (DNP), which transfers the high spin polarization of unpaired electrons to neighboring nuclei by microwave irradiation. This has been shown to be capable of enhancing the MR signal of $^{13}C$ NMR by more than a factor 40,000. Brindle's group has recently measured tumor pH with hyperpolarized $^{13}C$ bicarbonate (38). A Henderson-Hasselbach equation was used to calculate tissue pH from the voxel-wise ratio of $H^{13}CO_3^-$ to $^{13}CO_2$ following injection of hyperpolarized $H^{13}CO_3^-$. The measurement showed the pH (pHi and pHe) of a lymphoma xenograft was significantly lower (6.7± 0.1) than the surrounding normal tissue (7.1 ± 0.1). Although the dynamic pharmacokinetic distribution of bicarbonate results in an unclear average of pHi and pHe (39), the data were compared to that of 3-APP, suggesting that the majority of the $^{13}C$ signal was extracellular. A limitation of this approach is the rapid signal loss due to decay of the polarization. The T1 relaxation severely restricts the number of phase encoding samples during short acquisition times, as result in limited spatial resolution. However, a fast pulse sequence combined with compressed sensing reconstruction can partially compensate for this limitation.

## Magnetic resonance imaging (MRI)

**MR relaxometry—**Gadolinium (III) complexes are typically used as MRI contrast agents because they are the most efficient of all lanthanide ions at relaxing bulk water protons. Gadolinium-based agents primarily increase relaxivity via T1 mechanisms (1/R1) and hence result in increased signal intensity. It is possible to measure the tissue pH based on perturbing the relaxivity of water via pH-sensitive relaxation agents using MRI. One clever approach to measure pH used a polyion complex (PIC) consisting 30 Gd (III) chelates bound to a poly-ornithine chain (40). The packing conformation of this complex was pH-dependent leading to changes in water accessibility and correlation times and hence changes in R1 relaxivity. Independently, Sherry and Aime groups have synthesized gadolinium-based pH-sensitive agents whose relaxivities are pH-dependent (41,42). For one of these, GdDOTA-4AmP$^{5-}$, it has been shown that the H-bonding network created by phosphonate

side arm protonation provides a catalytic pathway for hydrogen exchange, making the longitudinal water proton relaxivity of this molecule pH-sensitive. Quantification of this measurement is highly dependent on accurate measurement of agent concentration in each imaging voxel (43). Raghunand et al. solved this using a two-phase injection method, involving two different gadolinium agents whose relaxivities are pH-insenstive and –sensitive, respectively. This approach was used to imaging pH in kidneys (44) and later in rat brain glioma (45). An assumption was made that the two agents have identical pharmacokinetics and tissue biodistributions, the distribution of the pH-insensitive agent can be used to predict the concentration of the pH-sensitive agent. Although this approach was useful, it is time consuming and thus limited in its potential for clinical utility. A single injection method has been developed to overcome these drawbacks (46). The pH-sensitive T1 agent GdDOTA-4AmP$^{5-}$ was mixed in a cocktail with the pH-insensitive T2* agent, DyDOTP$^{5}$ and injected into rats bearing glioma tumors. The $\Delta R2^*$ effects were used to determine [DyDOTP$^{5-}$] which could be used to predict [Gd] according to their mix ratio. The concentration thus determined was used to convert $\Delta R1$ of the pH-sensitive CA to pHe maps (FIGURE 4). The primary advantage of this protocol over previous studies is the rapidity of the pHe measurement. A drawback is the need to perform the calibrations in vivo, as the $\Delta R2^*$ effects are caused by susceptibility changes, and these are tumor-dependent. Nonetheless, a high-resolution pHe map can be generated with acceptable propagated errors at relatively modest concentrations of contrast agents within 16 minutes after start of infusion. In principle, this method is capable of yielding pHe maps following a single bolus injection, which would be appropriate in a clinical setting.

**Chemical Exchange Saturation Transfer (CEST)—**A novel approach to measure tissue pH is based on pH-sensitive chemical exchange-dependent magnetization transfer. This effect can be described by a simple two pool chemical exchange model, wherein the magnetizations for a labile proton and bulk water are derived by two groups of Bloch equations coupled by chemical exchange (47). The process involves the effect of pre-saturation that is undergoing chemical exchange of a nucleus from one site to a chemically different site. When the rate of exchange is less than the difference in frequency between the exchanging proton and bulk water, a selective pre-saturation pulse saturates the exchangeable hydrogen on exogenous or endogenous compounds, result in the transfer of hydrogen saturation state into bulk water via chemical exchange, thereby reducing the available water signal detected in the imaging experiment. Besides several MRI parameters such as bulk water T1 and RF irradiation power, CEST contrast highly depends on pH, exchangeable site concentration, temperature and other factors influencing the chemical environment of the exchangeable protons. This provides an opportunity to investigate the in vivo pH using CEST effect. pH imaging has become a important direction for CEST and is being evaluated by many groups. For a pH measurement, the hydrogens exchange more slowly at low pH due to base catalysis of proton exchange. Hence, the intensity of the water resonance can be perturbed via pH-sensitive exchange between water protons and those of slowly exchanging ionizable groups. There are three main categories of CEST imaging: diamagnetic CEST (DIACEST), paramagnetic CEST (PARACEST) and amide proton transfer (APT). Wolff and Balaban [46] first demonstrated the possibility of DIACEST imaging in which RF saturation is transferred from exchangeable solute protons to water. Hwang et al introduced a method to obtain accurate chemical exchange rates between water and -NH protons in vivo by avoiding magnetization transfer signal losses for solvent suppression (48). Van Zijl and colleagues improved the signal sensitivity caused by pH changes between 5-10 ppm (49). At same time, Zhang et al and Aime et al reported several PARACEST agents containing both highly shifted pH-insensitive and pH-sensitive exchangeable protons by enlarging the frequency range of exchanging sites (50,51). Most recently Zhou et al. demonstrated an amide proton transfer (APT) effect that is based on the

magnetization exchange between bulk water and labile endogenous amide protons. Given this hydrogen exchange is exponentially proportional to physiological pH, the pH contrast can be generated by measuring the exchange rates. pH-sensitive APT imaging has served as a new metabolic biomarker to clinical imaging for brain tissue (52). A drawback to CEST imaging remains the high concentrations required (>10 mM) and the need for strong MR irradiation pulses for pre-saturation, which are limited by power deposition limitations, or SAR. Pagel's group has recently developed a new PARACEST agent, Yb-DO3A-oAA, with two pH-responsive CEST centers that have different MR frequencies and different dependencies on pH (53). This allows quantification without saturating irradiation and mitigates the SAR problem The ratio of the two PARACEST effects can be used measure the entire physiological range of pHe from 6.1-8.0 with acceptable RF powers.

## pH and Metastasis

### Low pH effect on different Stages of metastasis

Metastasis involves the dissemination of cancer cells from the primary tumor to distant organs. Although genetically heterogeneous, the stages of metastasis are common in all cancers. It involves detachment of cells from the primary tumor, local invasion following proteolysis of extracellular matrix, disruption of basement membrane, intravasation in to the blood stream to yield circulating tumor cells. Circulating tumor cells, CTCs, are commonly observed in metastatic carcinomas, with a mean value of 60 and a maximum of 23,000 CTCs per 7.5 mL (2). The absolute numbers and molecular phenotypes of CTCs have prognostic value (54). To form metastases, CTCs must extravasate from the blood vessels at a secondary site. Following extravasation, the metastatic cells either co-opt existing vasculature, or induce neoangiogenesis, which coincides with conversion from a micro- to a macrometastasis. Several methods are currently available to follow metastasis *in vivo*. A valuable technique is optical biolumenesce imaging, which is non-invasive and semi-quantitative. Tumor cells expressing luciferase can be monitored longitudinally, beginning at the time of injection. Thus, these images can monitor the incidence and progression of metastatic lesion, *Ex vivo* images can also be obtained at the end of experiment to confirm and quantify results (Figure 5)

pH has shown to affect most of the steps in the metastatic cascade, either directly or indirectly. One of the essential steps in the growth of primary tumors is generation of new blood vessels (angiogenesis). In some systems, low pH can promote angiogenesis through induction of angiogenic growth factors, such as IL-8 and VEGF. Although the data support a generalized acid stimulation of IL-8 production (55), the data for VEGF are more equivocal, with some systems showing acid stimulation of VEGF (56) and others showing acid inhibition (57). Acid pH inversely correlates with VEGF promoter activity in human glioblastoma cells *in vitro* and xenografts *in vivo,* the induction of VEGF in Glioblastoma cells is mediated by Ap-1 and apparently ERK1/2 MAPK is required (56,58). Matrix metaloproteases, MMPs, are a family of zinc –binding endopeptidases that play a critical role in tissue remodeling during wound healing and metastasis. Although they have pH optima near pH 7.0, they are secreted as pro-enzymes whose activity is regulated by their conversion to active proteolytic forms. Acid pH can promote the conversion of MMPs. Low pH pre-treatment of human melanoma cell lines (A-07, D12 and T22) promotes experimental pulmonary metastasis in athymic nude mice by upregulating the expression of the proteolytic enzymes MMP-2, MMP-9, cathepsin B and cathepsin L (59). We have observed that low pH induces the release of active cathepsin B from MDA-mb-231 breast cancer cells (unpublished). *In vitro,* melanoma cells maintained under acidic conditions showed a greater motility and increased invasion when re-acclimated to normal pH (60). Imaging Proteases in cancer using optical (both fluorescent and bioluminescence), Positron emission tomography (PET), magnetic resonance imaging (MRI), and single-photon

emission computed tomography (SPECT) was reviewed. Optical imaging and specifically fluorescent is by far the most widely used technique for imaging protease activity *in vivo* including cathepsin family, and the matrix metalloprotease (MMP) family. Most of the fluorescent probes used are called "activatable probes", which can change their optical properties after protease cleavage. They are stable *in vivo* and show high specific labeling (61,62). The effect of acidity on tumor cells intravasation and extravasation has been investigated. The mechanism(s) of extravasation are somewhat controversial, i.e. whether it occurs through lodging of circulating tumor cells in small vessels or whether there is an interaction with post-capillary endothelia followed by active extravasation (63). More recent data support the latter hypothesis. Real-time intravital microscopy of an intracranial window chamber has shown that metastases grew only after a successful active extravasation of single cancer cells from the blood stream into the brain parenchyma (64). Cells were observed in the process of extravasation with intra- and extravascular parts and a narrowing at the vascular wall, suggesting that the cells extravasated through fenestrae in the vascular wall. Acidity may play role in this process of extravasation. In orthotopic breast cancer xenografts, inhibition of tumor acidity by chronic sodium bicarbonate appeared to have a greater effect on extravasation and colonization compared with intravasation (65). The number of circulating tumor cells did not appear to be altered by the bicarbonate treatment, although this conclusion was tempered due to low numbers of circulating tumor cells in this system. In further studies, also it has also been observed that chronic alkalinization with bicarbonate or other buffers will inhibit the formation of experimental lung metastases following tail vein injection in some, but not all tumor models (unpublished).

## Epithelial to mesenchymal transition (EMT)

EMT is defined as the reversible change from non-motile epithelial cells to motile mesenchymal cells. This increases invasiveness via the disassembly of cell-to-cell contact, loss of cell polarity, and significant cytoskeletal reorganization. EMT plays a key role in tumor progression and metastasis, and is capable of inducing invasiveness in even normal mammary epithelia (66). Most studies of EMT have been performed *in vitro*, but a direct role of EMT *in vivo* has been demonstrated using a transgenic mouse model of (MYC-driven) mammary carcinogenesis (67). The hallmark of EMT is the inactivation of E-cadherin via transcriptional repression of the E-cadherin promoter, chromosomal deletion of the E-cadherin gene, or proteolytic cleavage of the E-cadherin protein (68). The binding of E-cadherin with catenins and actin cytoskeleton is essential for the formation of strong cell-cell adhesion and any event that perturbs this relationship leads to destabilization of cell-cell adhesion and reorganization of the actin cytoskeleton (69). Acid pHe induces c-Src dependent tyrosine phosphorylation of β Catenin, leading to decrease the binding of E-cadherin to β Catenin, and consequently can lead to an increase cell migration and invasion (70).

## Does acidosis or lactic acidosis impair anticancer immunity?

An additional component of the metastatic cascade is innate immunity. Cancer cells are synthesizing aberrant proteins which are presented via the major histocompatibility complex (MHC-I/II) and can be potent inducers of immune surveillance. However, by various mechanisms, cancers are known to inhibit immune function. Lactic and general acidosis can affect immune function. Lactic acid impairs immune function including inhibition of polymorphonuclear leukocytes, chemotaxis, respiratory activity, suppression of proliferation and cytokine production of human cytotoxic T lymphocytes, as well as the T- Cell response to tumor -associated antigen (71). On the other hand, acidic extracellular pH can suppress human a subset of cytolytic T cells acting like NK cells in a non–MHC-restricted manner (72). There is also evidence that low pHe impairs the T cell response to antigen *in vivo* (73). Tumor derived lactate and acidification can inhibit monocyte cytokine (e.g. tumor necrosis

factor) production by blocking lactate export and glycolysis efflux (74) . These observations suggest that inhibiting acidosis in tumors could restore immune cell function and anti-tumor response.

### Can inhibition of tumor acidity inhibit metastasis?

Acidosis is a commonly observed phenotype, a “hallmark”, of cancer and is thus an attractive therapeutic target. Targeted treatment with proton pump inhibitors disrupt transmembrane pH gradients and can inhibit growth in human B cell leukemia (75). Alternatively, acidosis can be inhibited directly with the ingestion of alkaline buffers, such as bicarbonate (76). Chronic tumor alkalization by bicarbonate reduced spontaneous and experimental tumor metastases in human breast and prostate cancer mouse models (65). These effects were not generalized, however, as fast-growing tumor cell lines showed resistance. Reaction diffusion models predict that other buffers with higher pKa should be more efficacious (77) and preliminary data indicate that alternative buffers can reduce experimental metastasis in a prostate cancer model.

## Conclusion

Solid tumors invariably contain volumes that are highly acidic. While a number of techniques have been developed to image pH in vivo, improvements are needed with higher spatial and temporal resolution and that can be applied in human patients. In animal models the more acidic tumors are more aggressive and there has long been thought that the low pH of tumors stimulated tumor progression and metastases. Recent data would appear to support this, as ingested buffers can neutralize tumor acidity and lead to a reduction in metastases. However, the mechanisms by which acidity inhibits metastasis are elusive. There are multiple steps of metastasis that could each exhibit pH-sensitivity. Newer tools of molecular and functional imaging will play an important role in identifying and characterizing these mechanisms.

## Abbreviations

| | |
|---|---|
| **EMT** | Epithelial to Mesenchymal transition |
| **pHe** | extracellular pH |
| **pHi** | intracellular pH |
| **MRS** | Magnetic resonance spectroscopy |
| **MRSI** | magnetic resonance spectroscopy imaging |
| **Pi** | inorganic phosphate |
| **3-APP** | 3-aminopropyl phosphonate |
| **IEPA** | 2-imidazole-1-yl-3-ethoxycarbonyl propionic acid |
| **DNP** | Dynamic Nuclear Hyperpolarization |
| **CEST** | Chemical Exchange Saturation Transfer |
| **APT** | amide proton transfer |
| **PARACEST** | paramagnetic CEST |

## References

1. Ruoslahti E. How cancer spreads. Scientific American. 1996; 275(3):72–77. [PubMed: 8701296]

2. Allard WJ, Matera J, Miller MC, Repollet M, Connelly MC, Rao C, Tibbe AG, Uhr JW, Terstappen LW. Tumor cells circulate in the peripheral blood of all major carcinomas but not in healthy subjects or patients with nonmalignant diseases. Clin Cancer Res. 2004; 10(20):6897–6904. [PubMed: 15501967]
3. Tannock IF, Rotin D. Acid pH in tumors and its potential for therapeutic exploitation. Cancer research. 1989; 49(16):4373–4384. [PubMed: 2545340]
4. Gatenby RA, Gawlinski ET. A reaction-diffusion model of cancer invasion. Cancer research. 1996; 56(24):5745–5753. [PubMed: 8971186]
5. Stubbs M, McSheehy PM, Griffiths JR, Bashford CL. Causes and consequences of tumour acidity and implications for treatment. Mol Med Today. 2000; 6(1):15–19. [PubMed: 10637570]
6. Dellian M, Helmlinger G, Yuan F, Jain RK. Fluorescence ratio imaging of interstitial pH in solid tumours: effect of glucose on spatial and temporal gradients. British journal of cancer. 1996; 74(8): 1206–1215. [PubMed: 8883406]
7. Jahde E, Rajewsky MF. Tumor-selective modification of cellular microenvironment in vivo: effect of glucose infusion on the pH in normal and malignant rat tissues. Cancer research. 1982; 42(4): 1505–1512. [PubMed: 7060023]
8. Volk T, Jahde E, Fortmeyer HP, Glusenkamp KH, Rajewsky MF. pH in human tumour xenografts: effect of intravenous administration of glucose. British journal of cancer. 1993; 68(3):492–500. [PubMed: 8353039]
9. Jain RK, Shah SA, Finney PL. Continuous noninvasive monitoring of pH and temperature in rat Walker 256 carcinoma during normoglycemia and hyperglycemia. Journal of the National Cancer Institute. 1984; 73(2):429–436. [PubMed: 6589435]
10. Mazzio EA, Smith B, Soliman KF. Evaluation of endogenous acidic metabolic products associated with carbohydrate metabolism in tumor cells. Cell Biol Toxicol. 2009
11. Walenta S, Wetterling M, Lehrke M, Schwickert G, Sundfor K, Rofstad EK, Mueller-Klieser W. High lactate levels predict likelihood of metastases, tumor recurrence, and restricted patient survival in human cervical cancers. Cancer research. 2000; 60(4):916–921. [PubMed: 10706105]
12. Schwickert G, Walenta S, Sundfor K, Rofstad EK, Mueller-Klieser W. Correlation of high lactate levels in human cervical cancer with incidence of metastasis. Cancer research. 1995; 55(21):4757–4759. [PubMed: 7585499]
13. Newell K, Franchi A, Pouyssegur J, Tannock I. Studies with glycolysis-deficient cells suggest that production of lactic acid is not the only cause of tumor acidity. Proc Natl Acad Sci U S A. 1993; 90(3):1127–1131. [PubMed: 8430084]
14. Helmlinger G, Sckell A, Dellian M, Forbes NS, Jain RK. Acid production in glycolysis-impaired tumors provides new insights into tumor metabolism. Clin Cancer Res. 2002; 8(4):1284–1291. [PubMed: 11948144]
15. Robergs RA, Ghiasvand F, Parker D. Biochemistry of exercise-induced metabolic acidosis. Am J Physiol Regul Integr Comp Physiol. 2004; 287(3):R502–516. [PubMed: 15308499]
16. Gatenby RA, Gillies RJ. Why do cancers have high aerobic glycolysis? Nature reviews. 2004; 4(11):891–899.
17. Svastova E, Hulikova A, Rafajova M, Zat'ovicova M, Gibadulinova A, Casini A, Cecchi A, Scozzafava A, Supuran CT, Pastorek J, Pastorekova S. Hypoxia activates the capacity of tumor-associated carbonic anhydrase IX to acidify extracellular pH. FEBS letters. 2004; 577(3):439–445. [PubMed: 15556624]
18. Chen JL, Lucas JE, Schroeder T, Mori S, Wu J, Nevins J, Dewhirst M, West M, Chi JT. The genomic analysis of lactic acidosis and acidosis response in human cancers. PLoS Genet. 2008; 4(12):e1000293. [PubMed: 19057672]
19. Walenta S, Schroeder T, Mueller-Klieser W. Lactate in solid malignant tumors: potential basis of a metabolic classification in clinical oncology. Current medicinal chemistry. 2004; 11(16):2195–2204. [PubMed: 15279558]
20. Gillies RJ, Raghunand N, Garcia-Martin ML, Gatenby RA. pH imaging. A review of pH measurement methods and applications in cancers. IEEE Eng Med Biol Mag. 2004; 23(5):57–64.
21. Zhang X, Lin Y, Gillies RJ. Tumor pH and Its Measurement. J Nucl Med. 2010; 51(8):1167–1170. [PubMed: 20660380]

22. Gillies RJ, Liu Z, Bhujwalla Z. 31P-MRS measurements of extracellular pH of tumors using 3-aminopropylphosphonate. Am J Physiol. 1994; 267(1 Pt 1):C195–203. [PubMed: 8048479]

23. Soto GE, Zhu Z, Evelhoch JL, Ackerman JJ. Tumor 31P NMR pH measurements in vivo: a comparison of inorganic phosphate and intracellular 2-deoxyglucose-6-phosphate as pHnmr indicators in murine radiation-induced fibrosarcoma-1. Magnetic resonance in medicine : official journal of the Society of Magnetic Resonance in Medicine / Society of Magnetic Resonance in Medicine. 1996; 36(5):698–704. [PubMed: 8916020]

24. Gillies RJ, Ogino T, Shulman RG, Ward DC. 31P nuclear magnetic resonance evidence for the regulation of intracellular pH by Ehrlich ascites tumor cells. The Journal of cell biology. 1982; 95(1):24–28. [PubMed: 7142288]

25. Madden A, Glaholm J, Leach MO. An assessment of the sensitivity of in vivo 31P nuclear magnetic resonance spectroscopy as a means of detecting pH heterogeneity in tumours: a simulation study. The British journal of radiology. 1990; 63(746):120–124. [PubMed: 2310904]

26. Szwergold BS. NMR spectroscopy of cells. Annu Rev Physiol. 1992; 54:775–798. [PubMed: 1562190]

27. Bhujwalla ZM, McCoy CL, Glickson JD, Gillies RJ, Stubbs M. Estimations of intra- and extracellular volume and pH by 31P magnetic resonance spectroscopy: effect of therapy on RIF-1 tumours. Br J Cancer. 1998; 78(5):606–611. [PubMed: 9744499]

28. Raghunand N, Altbach MI, van Sluis R, Baggett B, Taylor CW, Bhujwalla ZM, Gillies RJ. Plasmalemmal pH-gradients in drug-sensitive and drug-resistant MCF-7 human breast carcinoma xenografts measured by 31P magnetic resonance spectroscopy. Biochem Pharmacol. 1999; 57(3): 309–312. [PubMed: 9890558]

29. Hunjan S, Mason RP, Mehta VD, Kulkarni PV, Aravind S, Arora V, Antich PP. Simultaneous intracellular and extracellular pH measurement in the heart by 19F NMR of 6-fluoropyridoxol. Magn Reson Med. 1998; 39(4):551–556. [PubMed: 9543416]

30. Ojugo AS, McSheehy PM, McIntyre DJ, McCoy C, Stubbs M, Leach MO, Judson IR, Griffiths JR. Measurement of the extracellular pH of solid tumours in mice by magnetic resonance spectroscopy: a comparison of exogenous (19)F and (31)P probes. NMR Biomed. 1999; 12(8): 495–504. [PubMed: 10668042]

31. Rabenstein DL, Isab AA. Determination of the intracellular pH of intact erythrocytes by 1H NMR spectroscopy. Anal Biochem. 1982; 121(2):423–432. [PubMed: 7103074]

32. Gil S, Zaderenzo P, Cruz F, Cerdán S, Ballesteros P. Imidazol-1-ylalkanoic acids as extrinsic 1H NMR probes for the determination of intracellular pH, extracellular pH and cell volume. Bioorg Med Chem. 1994; 2(5):305–314. [PubMed: 7922141]

33. van Sluis R, Bhujwalla ZM, Raghunand N, Ballesteros P, Alvarez J, Cerdan S, Galons JP, Gillies RJ. In vivo imaging of extracellular pH using 1H MRSI. Magn Reson Med. 1999; 41(4):743–750. [PubMed: 10332850]

34. Garcia-Martin ML, Herigault G, Remy C, Farion R, Ballesteros P, Coles JA, Cerdan S, Ziegler A. Mapping extracellular pH in rat brain gliomas in vivo by 1H magnetic resonance spectroscopic imaging: comparison with maps of metabolites. Cancer research. 2001; 61(17):6524–6531. [PubMed: 11522650]

35. Provent P, Benito M, Hiba B, Farion R, Lopez-Larrubia P, Ballesteros P, Remy C, Segebarth C, Cerdan S, Coles JA, Garcia-Martin ML. Serial in vivo spectroscopic nuclear magnetic resonance imaging of lactate and extracellular pH in rat gliomas shows redistribution of protons away from sites of glycolysis. Cancer research. 2007; 67(16):7638–7645. [PubMed: 17699768]

36. Hoffman DW, Henkens RW. The rates of fast reactions of carbon dioxide and bicarbonate in human erythrocytes measured by carbon-13 NMR. Biochem Biophys Res Commun. 1987; 143(1): 67–73. [PubMed: 3103622]

37. Arús C, Chang YC, Bárány M. The separation of phosphocreatine from creatine, and pH determination in frog muscle by natural abundance 13C-NMR. Biochim Biophys Acta. 1985; 844(1):91–93. [PubMed: 3871336]

38. Gallagher FA, Kettunen MI, Day SE, Hu DE, Ardenkjaer-Larsen JH, Zandt R, Jensen PR, Karlsson M, Golman K, Lerche MH, Brindle KM. Magnetic resonance imaging of pH in vivo

using hyperpolarized 13C-labelled bicarbonate. Nature. 2008; 453(7197):940–943. [PubMed: 18509335]

39. Schroeder MA, Swietach P, Atherton HJ, Gallagher FA, Lee P, Radda GK, Clarke K, Tyler DJ. Measuring intracellular pH in the heart using hyperpolarized carbon dioxide and bicarbonate: a 13C and 31P magnetic resonance spectroscopy study. Cardiovasc Res. 2010; 86(1):82–91. [PubMed: 20008827]
40. Mikawa M, Miwa N, Bräutigam M, Akaike T, Maruyama A. Gd(3+)-loaded polyion complex for pH depiction with magnetic resonance imaging. J Biomed Mater Res. 2000; 49(3):390–395. [PubMed: 10602072]
41. Lowe MP, Parker D, Reany O, Aime S, Botta M, Castellano G, Gianolio E, Pagliarin R. pH-dependent modulation of relaxivity and luminescence in macrocyclic gadolinium and europium complexes based on reversible intramolecular sulfonamide ligation. Journal of the American Chemical Society. 2001; 123(31):7601–7609. [PubMed: 11480981]
42. Zhang S, Wu K, Sherry A. A Novel pH-Sensitive MRI Contrast Agent. Angew Chem Int Ed Engl. 1999; 38(21):3192–3194. [PubMed: 10556899]
43. Beauregard, DA.; Parker, D.; Brindle, KM. Relaxation-based mapping of tumour pH. Proceedings of the 6th Annual Meeting of ISMRM; 1998. p. 53
44. Raghunand N, Howison C, Sherry AD, Zhang S, Gillies RJ. Renal and systemic pH imaging by contrast-enhanced MRI. Magnetic resonance in medicine : official journal of the Society of Magnetic Resonance in Medicine / Society of Magnetic Resonance in Medicine. 2003; 49(2):249–257. [PubMed: 12541244]
45. Garcia-Martin ML, Martinez GV, Raghunand N, Sherry AD, Zhang S, Gillies RJ. High resolution pH(e) imaging of rat glioma using pH-dependent relaxivity. Magnetic resonance in medicine : official journal of the Society of Magnetic Resonance in Medicine / Society of Magnetic Resonance in Medicine. 2006; 55(2):309–315. [PubMed: 16402385]
46. Zhang, X.; Martinez, GV.; Garcia-Martin, ML.; Woods, M.; Sherry, D.; Gillies, RJ. High Spatio-Temporal Resolution pHe Mapping of a Rat Glioma Derived From pH-Dependent Spin-Lattice Relaxivity. Toronto, Ontario, Canada: May 3-9. 2008
47. Sherry AD, Woods M. Chemical exchange saturation transfer contrast agents for magnetic resonance imaging. Annu Rev Biomed Eng. 2008; 10:391–411. [PubMed: 18647117]
48. Hwang TL, van Zijl PC, Mori S. Accurate quantitation of water-amide proton exchange rates using the phase-modulated CLEAN chemical EXchange (CLEANEX-PM) approach with a Fast-HSQC (FHSQC) detection scheme. J Biomol NMR. 1998; 11(2):221–226. [PubMed: 9679296]
49. Snoussi K, Bulte JWM, Guéron M, van Zijl PCM. Sensitive CEST agents based on nucleic acid imino proton exchange: detection of poly(rU) and of a dendrimer-poly(rU) model for nucleic acid delivery and pharmacology. Magnetic resonance in medicine : official journal of the Society of Magnetic Resonance in Medicine / Society of Magnetic Resonance in Medicine. 2003; 49(6):998–1005. [PubMed: 12768576]
50. Zhang S, Merritt M, Woessner DE, Lenkinski RE, Sherry AD. PARACEST agents: modulating MRI contrast via water proton exchange. Acc Chem Res. 2003; 36(10):783–790. [PubMed: 14567712]
51. Aime S, Barge A, Delli Castelli D, Fedeli F, Mortillaro A, Nielsen FU, Terreno E. Paramagnetic lanthanide(III) complexes as pH-sensitive chemical exchange saturation transfer (CEST) contrast agents for MRI applications. Magnetic resonance in medicine : official journal of the Society of Magnetic Resonance in Medicine / Society of Magnetic Resonance in Medicine. 2002; 47(4):639–648. [PubMed: 11948724]
52. Zhou J, Lal B, Wilson DA, Laterra J, van Zijl PCM. Amide proton transfer (APT) contrast for imaging of brain tumors. Magnetic resonance in medicine : official journal of the Society of Magnetic Resonance in Medicine / Society of Magnetic Resonance in Medicine. 2003; 50(6):1120–1126. [PubMed: 14648559]
53. Liu, G.; Li, Y.; Pagel, M. Measurement of Extracelluar pH Using A Single MRI Contrast Agent Based On PARACEST Effects. 2007.
54. Resel Folkersma L, Olivier Gomez C, San Jose Manso L, Veganzones de Castro S, Galante Romo I, Vidaurreta Lazaro M, de la Orden GV, Arroyo Fernandez M, Diaz Rubio E, Silmi Moyano A,

Maestro de Las Casas MA. Immunomagnetic Quantification of Circulating Tumoral Cells in Patients with Prostate Cancer: Clinical and Pathological Correlation. Archivos espanoles de urologia. 63(1):23–31. [PubMed: 20157216]

55. Xu L, Fidler IJ. Acidic pH-induced elevation in interleukin 8 expression by human ovarian carcinoma cells. Cancer research. 2000; 60(16):4610–4616. [PubMed: 10969814]
56. Fukumura D, Xu L, Chen Y, Gohongi T, Seed B, Jain RK. Hypoxia and acidosis independently up-regulate vascular endothelial growth factor transcription in brain tumors in vivo. Cancer research. 2001; 61(16):6020–6024. [PubMed: 11507045]
57. Scott PA, Gleadle JM, Bicknell R, Harris AL. Role of the hypoxia sensing system, acidity and reproductive hormones in the variability of vascular endothelial growth factor induction in human breast carcinoma cell lines. International journal of cancer. 1998; 75(5):706–712.
58. Xu L, Fukumura D, Jain RK. Acidic extracellular pH induces vascular endothelial growth factor (VEGF) in human glioblastoma cells via ERK1/2 MAPK signaling pathway: mechanism of low pH-induced VEGF. The Journal of biological chemistry. 2002; 277(13):11368–11374. [PubMed: 11741977]
59. Rofstad EK, Mathiesen B, Kindem K, Galappathi K. Acidic extracellular pH promotes experimental metastasis of human melanoma cells in athymic nude mice. Cancer research. 2006; 66(13):6699–6707. [PubMed: 16818644]
60. Moellering RE, Black KC, Krishnamurty C, Baggett BK, Stafford P, Rain M, Gatenby RA, Gillies RJ. Acid treatment of melanoma cells selects for invasive phenotypes. Clinical & experimental metastasis. 2008; 25(4):411–425. [PubMed: 18301995]
61. Blum G, von Degenfeld G, Merchant MJ, Blau HM, Bogyo M. Noninvasive optical imaging of cysteine protease activity using fluorescently quenched activity-based probes. Nat Chem Biol. 2007; 3(10):668–677. [PubMed: 17828252]
62. Yang Y, Hong H, Zhang Y, Cai W. Molecular Imaging of Proteases in Cancer. Cancer Growth Metastasis. 2009; 2:13–27. [PubMed: 20234801]
63. Fidler IJ. Cancer metastasis. Br Med Bull. 1991; 47(1):157–177. [PubMed: 1863845]
64. Kienast Y, von Baumgarten L, Fuhrmann M, Klinkert WE, Goldbrunner R, Herms J, Winkler F. Real-time imaging reveals the single steps of brain metastasis formation. Nature medicine. 16(1): 116–122.
65. Robey IF, Baggett BK, Kirkpatrick ND, Roe DJ, Dosescu J, Sloane BF, Hashim AI, Morse DL, Raghunand N, Gatenby RA, Gillies RJ. Bicarbonate increases tumor pH and inhibits spontaneous metastases. Cancer research. 2009; 69(6):2260–2268. [PubMed: 19276390]
66. Blick T, Widodo E, Hugo H, Waltham M, Lenburg ME, Neve RM, Thompson EW. Epithelial mesenchymal transition traits in human breast cancer cell lines. Clinical & experimental metastasis. 2008; 25(6):629–642. [PubMed: 18461285]
67. Trimboli AJ, Fukino K, de Bruin A, Wei G, Shen L, Tanner SM, Creasap N, Rosol TJ, Robinson ML, Eng C, Ostrowski MC, Leone G. Direct evidence for epithelial-mesenchymal transitions in breast cancer. Cancer research. 2008; 68(3):937–945. [PubMed: 18245497]
68. Agiostratidou G, Hulit J, Phillips GR, Hazan RB. Differential cadherin expression: potential markers for epithelial to mesenchymal transformation during tumor progression. Journal of mammary gland biology and neoplasia. 2007; 12(2-3):127–133. [PubMed: 17564818]
69. Guarino M, Rubino B, Ballabio G. The role of epithelial-mesenchymal transition in cancer pathology. Pathology. 2007; 39(3):305–318. [PubMed: 17558857]
70. Chen KH, Tung PY, Wu JC, Chen Y, Chen PC, Huang SH, Wang SM. An acidic extracellular pH induces Src kinase-dependent loss of beta-catenin from the adherens junction. Cancer letters. 2008; 267(1):37–48. [PubMed: 18423982]
71. Fischer K, Hoffmann P, Voelkl S, Meidenbauer N, Ammer J, Edinger M, Gottfried E, Schwarz S, Rothe G, Hoves S, Renner K, Timischl B, Mackensen A, Kunz-Schughart L, Andreesen R, Krause SW, Kreutz M. Inhibitory effect of tumor cell-derived lactic acid on human T cells. Blood. 2007; 109(9):3812–3819. [PubMed: 17255361]
72. Fischer B, Muller B, Fisch P, Kreutz W. An acidic microenvironment inhibits antitumoral non-major histocompatibility complex-restricted cytotoxicity: implications for cancer immunotherapy. J Immunother. 2000; 23(2):196–207. [PubMed: 10746546]

73. Bosticardo M, Ariotti S, Losana G, Bernabei P, Forni G, Novelli F. Biased activation of human T lymphocytes due to low extracellular pH is antagonized by B7/CD28 costimulation. European journal of immunology. 2001; 31(9):2829–2838. [PubMed: 11536182]

74. Dietl K, Renner K, Dettmer K, Timischl B, Eberhart K, Dorn C, Hellerbrand C, Kastenberger M, Kunz-Schughart LA, Oefner PJ, Andreesen R, Gottfried E, Kreutz MP. Lactic acid and acidification inhibit TNF secretion and glycolysis of human monocytes. J Immunol. 184(3):1200–1209. [PubMed: 20026743]

75. De Milito A, Canese R, Marino ML, Borghi M, Iero M, Villa A, Venturi G, Lozupone F, Iessi E, Logozzi M, Mina PD, Santinami M, Rodolfo M, Podo F, Rivoltini L, Fais S. pH-dependent antitumor activity of proton pump inhibitors against human melanoma is mediated by inhibition of tumor acidity. Int J Cancer. 2009

76. Raghunand N, He X, van Sluis R, Mahoney B, Baggett B, Taylor CW, Paine-Murrieta G, Roe D, Bhujwalla ZM, Gillies RJ. Enhancement of chemotherapy by manipulation of tumour pH. British journal of cancer. 1999; 80(7):1005–1011. [PubMed: 10362108]

77. Silva AS, Yunes JA, Gillies RJ, Gatenby RA. The potential role of systemic buffers in reducing intratumoral extracellular pH and acid-mediated invasion. Cancer research. 2009; 69(6):2677–2684. [PubMed: 19276380]

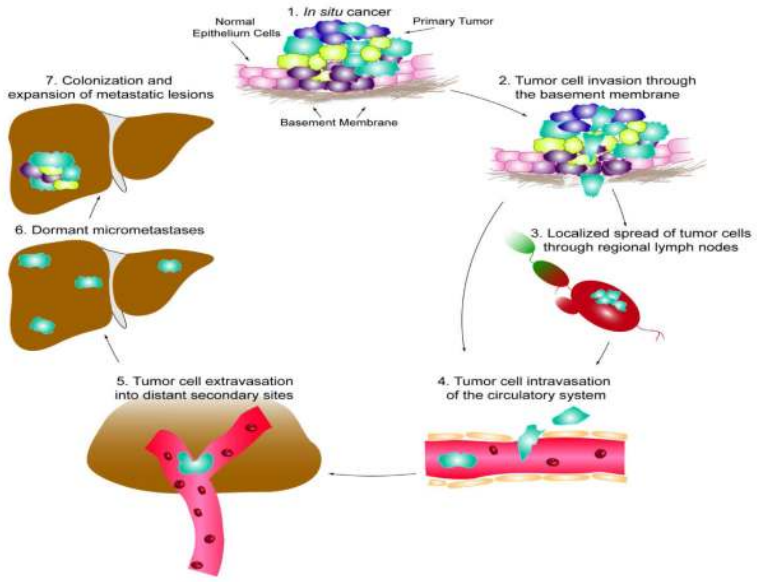


**Figure 1. Stages of Metastasis**

Primary carcinomas arise from epithelia which face ductal lumens and are separated from stroma by a basement membrane. After disruption of basement membrane integrity the locally invasive cells gain access to lymphatic- and heme-vasculature wherein they form circulating tumor cells, CTCs. At secondary sites (right) the tumor cells extravasate into parenchyma, where they colonize and become vascularized either through co-option or neo-angiogenesis (reprinted by permission. Scientific American.)

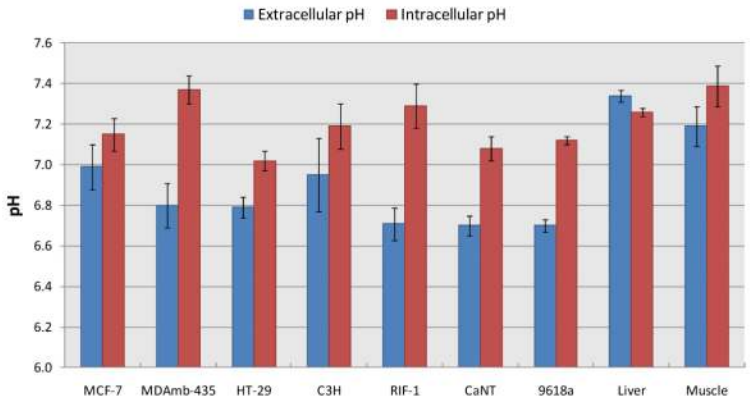


**Figure 2. pHe and pHi of tumors and normal tissues by 31P MRS of 3-APP and Pi respectively**
Subsequent measurements have shown unequivocally that the pHe of tumor xenografts is acidic, whereas the pHi is neutral-to-alkaline.

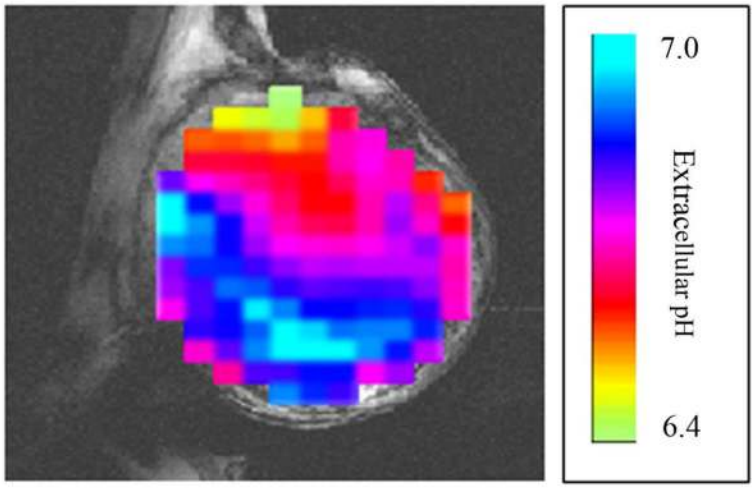


**Figure 3. pHe map of breast cancer xenograft**

MDA-mb-435 flank tumors were infused with IEPA and pH was measured by 1H MRS.

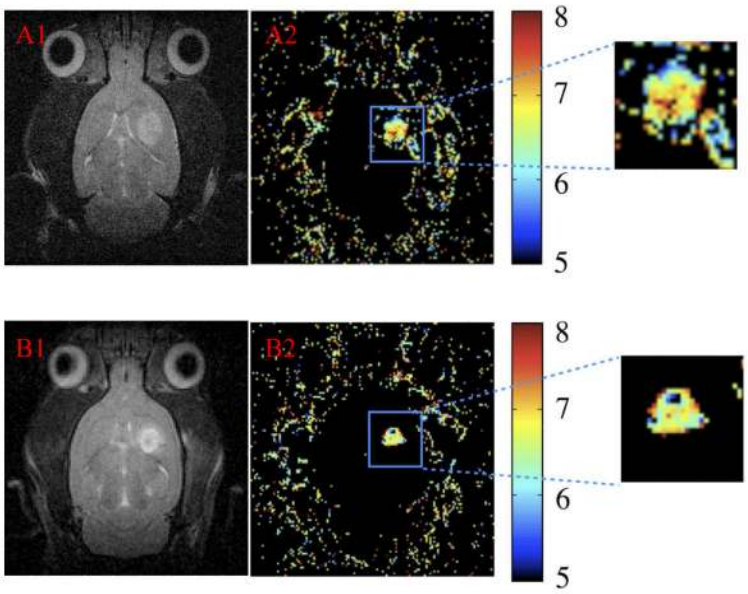


**Figure 4.**

In vivo tumor pHe maps were generated using relaxivity-based single injection method, a combination of T1-weighted imaging and spectroscopic imaging in a C6 rat glioma model. A1 and B1 shows T1-W contrast enhancement after CA infusion in two different animals. A2 and B2 are the corresponding tumor pHe maps.

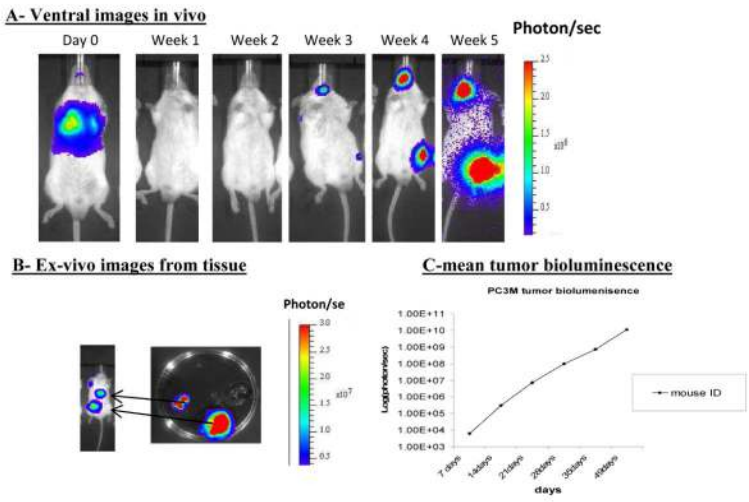


**Figure 5. Measurement of metastasis in vivo and in vitro**

Experimental Metastases in Intravenous Model - SCID-beige injected with5×10 6 of PC-3M-luc-C6 cells. **A**. Lung signals are visible after cell injection on day 0. Signals drop as lungs clear between day 1 to week 2. Metastatic signals reappear in week 3-4 and all mice develop multiple signals by week 5. **B.** Ex vivo imaging confirms metastases in bone and lungs. **C.** tumor bioluminescence expressed as photons/sec.

## TABLE 1

Indicators for measurement of pH in vivo with MRS(I) .

| Isotope | Frequency (rel 1H) | % Natural abundance | Sensitivity (rel 1H) | Compounds | Application |
|---|---|---|---|---|---|
| $^{1}H$ | 1.00 | 99.98 | 100 | 2-imidazole-1-yl-3-ethoxycarbonylpropionic acid (IEPA) | pHe |
| $^{19}F$ | 0.94 | 100 | 83 | 3-[N-(4-fluor-2-trifluoromethylphenyl)-sulphamoyl]-propionic acid (ZK-150471) | pHe |
| | | | | Vitamin B6 derivatives | pHi pHe |
| $^{31}P$ | 0.41 | 100 | 6.6 | Inorganic phosphate (Pi) | pHi |
| | | | | 3-aminopropylphosphonate (3-APP) | pHe |
| $^{13}C$ | 0.25 | 1.1 | 0.016 | Hyperpolarized $^{13}C$-labelled bicarbonate | pHe |